Hyperfine-Field-Mediated Spin Beating in Electrostatically Bound Charge Carrier Pairs

D. R. McCamey, K. J. van Schooten, W. J. Baker, S.-Y. Lee, S.-Y. Paik, J. M. Lupton,* and C. Boehme†

Department of Physics and Astronomy, University of Utah, 115 South 1400 East, Salt Lake City, Utah 84112, USA

(Received 16 June 2009; published 8 January 2010)

Organic semiconductors offer a unique environment to probe the hyperfine coupling of electronic spins to a nuclear spin bath. We explore the interaction of spins in electron-hole pairs in the presence of inhomogeneous hyperfine fields by monitoring the modulation of the current through an organic light emitting diode under *coherent* spin-resonant excitation. At weak driving fields, only one of the two spins in the pair precesses. As the driving field exceeds the difference in local hyperfine field experienced by electron and hole, both spins precess, leading to pronounced spin beating in the transient Rabi flopping of the current. We use this effect to measure the magnitude and spatial variation in hyperfine field on the scale of single carrier pairs, as required for evaluating models of organic magnetoresistance, improving organic spintronics devices, and illuminating spin decoherence mechanisms.

DOI: 10.1103/PhysRevLett.104.017601 PACS numbers: 76.30.−v, 73.61.Ph

The hyperfine interaction between single electronic and nuclear spins is well understood theoretically [1]. In real condensed matter spin-based systems, however, individual electronic spins couple to an ensemble, or bath, of nuclear spins [2–4]. Such coupling is of both technological and fundamental importance. Local variations in the hyperfine field contribute significantly to spin dephasing in many types of quantum bits, including GaAs quantum dots [2,5,6] and NV centers in diamond [6]. As well as influencing the fundamental recombination processes responsible for light emission in organic light-emitting diodes (OLEDs), such local variations are also a leading candidate for explaining the large magnetoresistive effects observed in organic semiconductors [7–12]. For example, the bipolaron model of organic magnetoresistance proposes that spin mixing by local variations of the hyperfine field reduces spin blockade of hopping transport at low magnetic fields. The interaction of quantum systems with their environment has also been discussed in the context of the emergence of classical behavior [13].

Exploiting spin-dependent carrier recombination in organic semiconductors [14], we probe the fundamental spin interaction within pairs of electrostatically bound charge carriers, as mediated by the local nuclear spin bath. We demonstrate *time-domain beating* in the spin precession in electrostatically correlated spin pairs in an OLED, driven by a resonant electromagnetic field. Such beating occurs when the driving field compensates the local difference in hyperfine fields acting on each spin within a pair, and appears as a doubling of the frequency with which the spin pair transitions between singlet and triplet configuration [15,16]. Organic semiconductors provide a unique platform to explore the underlying physics of spin coupling due to long spin lifetimes, weak spin-orbit coupling, and facile electric readout [14].

While usually considered as a way to obtain promising new device architectures [17,18], organic spin electronics provide a rich parameter space in which to study fundamental spin physics [19]. We recently demonstrated that conventional disordered organic semiconductors, such as the conjugated polymer poly[2-methoxy-5-(2′-ethyl-hexyloxy)-1,4-phenylene vinylene] (MEH-PPV), display surprisingly long spin coherence times on the order of 1 μs, which can readily be exploited using pulsed electrically detected magnetic resonance (PEDMR) techniques [14]. As with other carbon-based systems such as fullerenes [20], carbon nanotubes [3,21], graphene [22], and diamond [4], organic semiconductors can exhibit extremely weak spin-orbit coupling; however, the ubiquitous hydrogen atoms in organic semiconductors give rise to significant hyperfine interactions, which, combined with the structural disorder, result in substantial inhomogeneous broadening of resonance field strengths [23]. Organic semiconductors are inherently large-gap ambipolar materials and can support both electron and hole currents in the undoped state [24], which, combined with the weak dielectric screening and strong carrier pair correlation, allows us to probe intrinsic spin interactions in electrostatically coupled electron-hole pairs. In contrast to mesoscopic systems, which are conventionally used to study elementary spin physical processes [2,5,25], organic semiconductors combine facile processing with a wide range of physical interactions. Rather than selecting particular spin coupling scenarios by addressing individual units, as is the approach commonly pursued in quantum dot spin spectroscopy [2,5], disordered strongly interacting conjugated polymers allow us to use PEDMR to select particular interaction pathways. We are thus able to investigate the transition of electrostatically bound charge carrier pairs from acting as isolated charges (with a spin-1/2 resonance) to displaying correlated behavior.

Under standard operating conditions of an OLED, electrons and holes are injected from opposite electrodes, migrate through the device, and ultimately recombine, forming either a light-emitting exciton of singlet character or a non-light-emitting triplet exciton (referred to here as

injection-recombination). As the injected charge carriers move through the disordered organic semiconductor film, two characteristic distances can be defined: r_C, the carrier separation below which the Coulombic binding energy of electron and hole exceeds the thermal energy of the carriers, and r_K, the carrier separation below which the electrostatically bound carrier spins begin to interact. Below r_K a linear superposition of the spin states has to be considered, leading to an energetic splitting between singlet and triplet manifolds [26].

Generally, experiments on OLEDs probe either injection-recombination or the reverse process: dissociation of an optically generated exciton to yield a photocurrent. Very little is known about the interchromophoric exchange interaction, when electron and hole reside on different conjugated segments (on different chains or within a chain) within the film. In contrast, when electron and hole finally recombine on one conjugated segment, the resulting singlet or triplet excitons are strongly exchange split by typically 0.7 eV [9]. Coherent spin effects allow us to investigate this important transition region at the onset of intermolecular exchange. As singlet excitons are typically preferable for efficient OLEDs, it is especially crucial to understand the nature of this exchange to appreciate fundamental efficiency limitations in devices [27].

We performed PEDMR [28] on MEH-PPV OLEDs [29] similar to devices previously described [14]. In those earlier experiments, noise-limited current resolution prohibited observation of the intricacies of the resonance line shape [30], which was assumed to originate from single carriers, either electrons or holes. Figure 1 shows the change in current passing through an operating OLED biased in the forward direction as a function of magnetic field (B_0), following a short microwave pulse. Careful inspection of the signal reveals that it cannot be fit by a single Gaussian line, as would be expected for a resonance from a single spin species (see supporting information for further discussion [31]). The data are well fit by both two and three Gaussian resonances. This corresponds to a system with two spin species which couple to different numbers of surrounding nuclear spins (two lines), or a system with reasonable exchange coupling between the two spins (three lines). Earlier studies have, however, demonstrated that the resonance shape in fact arises from the difference in local hyperfine field felt by each spin [30,32], indicating that this is the dominant cause of the observed spectra; additional reasons for discounting exchange coupling are given in the supplementary information [31,33]. The ability to fit the spectrum with two Gaussian lines indicates that the signal arises from the two different spin species which form the electrostatically coupled carrier pair: electron and hole. When spin resonance causes coherent precession of either the electron or the hole spin in the driving microwave (B_1) field as illustrated in the inset of Fig. 1, the permutation symmetry of the spin pairs will start to oscillate at the same frequency [15], resulting in a change of the total recombination and

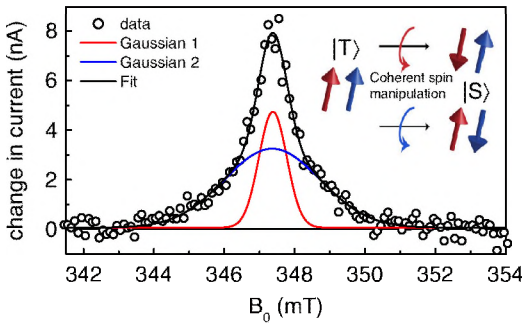

FIG. 1 (color online). Observation of the two spin partners in an electrostatically bound carrier pair in an OLED. The pair can be shuttled between the singlet and triplet manifold by coherently manipulating the orientation of one of the two electron spins within the pair (inset). The change in current through a MEH-PPV OLED 10.2 μs after a microwave pulse is plotted as a function of external magnetic field B_0. The spectrum is described by two Gaussian lines, which we assign to the two spins in the carrier pair. Further fit possibilities are discussed and discounted in the supporting information [31,33].

dissociation rates of the system. Indeed, it is this change of rates which allows electrical detection of the resonance, since it causes an increase in the free polaron density directly following the spin manipulation (see supplementary information in Ref. [14] for details of this mechanism).

The peak of the resonance line provides the g factor of the spin species, $g = 2.003$. This value is in agreement with previous conventional, optically detected, and electrically detected electron paramagnetic resonance (EPR) studies of radicals and radical pairs [30,34]. Since the width of the resonance Γ is not determined by spin-orbit coupling or dipolar electron spin interactions (discussed in more detail in the supplementary information [31]), it offers a measure of the distribution of the hyperfine field strength present at different sites in the disordered molecular film [23]. While we cannot assign positive and negative charges to the two lines observed, it is not surprising that Γ should differ for electrons and holes since this will depend very sensitively on the localization of the carrier wave function; the degree of localization determines the number of hydrogenic nuclear spins the carrier spin interacts with, which in turn need not be equal for the two charge species. The larger the number of nuclear spins which interact with the polaron, the smaller the total hyperfine field they will feel. This rather counterintuitive effect arises because the standard deviation (from zero) of the net nuclear spin orientation decreases as the ensemble size increases (due to the central limit theorem), leading us to conclude that the narrower line arises from the larger polaron.

Fitting two Gaussians, $G(B, \Gamma)$, to the resonance spectrum allows us to extract the hyperfine fields felt by each polaron type, $\Gamma_a = 2.7(2)$ mT and $\Gamma_b = 0.79(5)$ mT, analogous to earlier incoherent EDMR investigations [30]. We can also estimate the difference in hyperfine field between electron and hole within a carrier pair by computing the expectation value of the difference in a random

distribution of hyperfine fields, i.e., $\langle|\Delta B_{\rm hyp}|\rangle = \iint_{-\infty}^{+\infty} G_a(B_a,\Gamma_a)G_b(B_b,\Gamma_b)|B_a - B_b|dB_b dB_a = 1.1(1)$ mT. We note that the experimental value of $\langle|\Delta B_{\rm hyp}|\rangle$ obtained in this way is in agreement with earlier theoretical estimates based on the inhomogeneous line shape [10].

We present here an experiment that allows us to confirm this estimate by directly probing the difference in hyperfine field of spins within charge carrier pairs *coherently manipulated* with different B_1 driving fields. Figure 2(a) displays coherent modulation of the OLED current as a function of the duration of a spin-resonant microwave pulse of magnitude $B_1 = 1.2$ mT [35]. As the length of the pulse increases, the spin state of the charge carrier pair undergoes Rabi oscillations from singlet to triplet and back again, as sketched in the inset of Fig. 1. This oscillation leads to a periodic modulation of the current depending on the duration of the applied B_1 field. The oscillations, seen in Fig. 2(a), which extend for over 17 periods, can be accurately described by a superposition of two oscillating functions of frequency Ω and 2Ω. For comparison, a periodic function with a single period is fitted (dotted line). The high quality of the data and the long coherence time of the spin precession allow us to perform an accurate analysis of the Fourier components in the oscillations. Figure 2(b) shows the frequency spectrum for four different driving fields, B_1, close to the estimated field $\langle|\Delta B_{\rm hyp}|\rangle$. Two peaks are clearly identified in the Fourier spectrum, at $\Omega = \Omega_{\rm Rabi}$ and $\Omega = 2\Omega_{\rm Rabi}$). The Fourier frequency components are also plotted as a function of driving field B_1. As expected from Rabi's frequency equation for a spin in resonance with an electromagnetic field, the Rabi frequency varies linearly with B_1 field for both peaks [with a factor of 2 difference between slopes, lines in 2(b)]. The ratio of peak areas also changes as the B_1 field is changed, with the beat signal disappearing at low driving fields.

Figure 3(a) illustrates the Rabi nutation experiment. As long as $B_1 < |\Delta B_{\rm hyp}|$, either electron or hole spin within the pair should precess in response to the on-resonant driving field, but not both, as the other pair partner is likely out of resonance. Once $B_1 > |\Delta B_{\rm hyp}|$, the driving field is so strong that the intrinsic hyperfine field-induced variation between electron and hole resonance (g factor) is overcome, and both carriers within a pair precess *together* rather than individually [15,16]. This joint precession halves the time period required for triplet-singlet transitions, thereby doubling the frequency of modulation of the measured device current. Frequency doubling arises since the pair's spin permutation symmetries reflect the beat oscillation of the two pair partners' spin-1/2 Rabi frequencies (i.e., $\Omega = 2\Omega_{\rm Rabi}$) [15,16]. This dependence is summarized in Fig. 3(b), where the relative fraction of spin pairs with the fundamental ($\Omega_{\rm Rabi}$) and twice the fundamental frequency ($2\Omega_{\rm Rabi}$) [36] is plotted as a function of B_1. The B_1 dependence of the relative intensities of fundamental and harmonic frequencies can be accurately described by a quantile function, as expected given a Gaussian distribution, $G(\Gamma)$ of $|\Delta B_{\rm hyp}|$, i.e., $f(B_1) = 2\int_0^{B_1} G(\Gamma)dB$ where Γ is determined by $\langle|\Delta B_{\rm hyp}|\rangle$. The two fit curves cross at $B_1 = 1.1$ mT, precisely when the driving field overcomes the difference in hyperfine fields experienced by the electron and hole within a pair. By overcoming the local hyperfine field disorder at $B_1 = \langle|\Delta B_{\rm hyp}|\rangle$, a threshold driving field is reached at which the pair partners' resonances mix and spin beating occurs. This direct measurement of $\langle|\Delta B_{\rm hyp}|\rangle$ by the observation of B_1-induced spin beating coincides with our estimate based on the resonance line shapes shown in Fig. 1.

We note that the experiments presented here did not reveal signatures of spin-dipolar interactions within the pair, which would be manifested in either the magnetic field dependence of the resonance [31] or in the Rabi nutation as a component with frequency $\Omega = \sqrt{2}\Omega_{\rm Rabi}$ [37]. Spin-exchange coupling can also be excluded, since such coupling results in $f(2\Omega_{\rm Rabi}) = 1$ independent of the

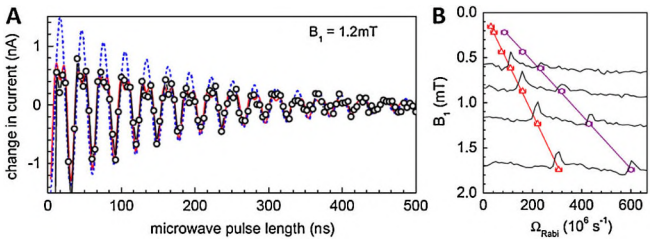

FIG. 2 (color online). (a) Coherent oscillations of the ensemble of spin pairs, observed by measuring the change in OLED current 7.2 μs after application of resonant microwave pulses of increasing length. The fit with an exponentially damped sinusoidal function with components at both $\Omega_{\rm Rabi}$ and $2\Omega_{\rm Rabi}$ is shown (solid red line), as is a fit with only a single frequency component $\Omega_{\rm Rabi}$ (dashed blue line). (b) Sample Fourier transform spectra of Rabi nutation traces obtained at different B_1 field strengths. The frequency of the two peaks was determined, and plotted as a function of B_1.

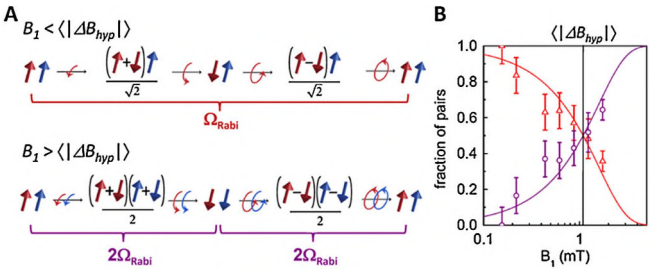

FIG. 3 (color online). Beating of spin precession following compensation of the difference in intrapair hyperfine fields. (a) As the driving field is increased, the current modulation frequency changes from the Rabi frequency $\Omega_{\rm Rabi}$ to twice the Rabi frequency. This doubling arises because the difference in intrapair hyperfine fields is overcome and both spins are simultaneously in resonance. (b) Relative fraction of pairs with $\Omega = \Omega_{\rm Rabi}$ (not beating) ($\triangle$) and $\Omega = 2\Omega_{\rm Rabi}$ (beating) ($\bigcirc$). The solid lines show the expected form of the distribution, the crossover of which gives a measure of $\langle|\Delta B_{\rm hyp}|\rangle = 1.1(1)$ mT.

magnitude of B_1 [31,33]. The absence of dipolar spin-spin interactions leads us to conclude that the carriers in a pair are separated by a distance of more than 2 nm, and are therefore most likely intermolecular.

Besides offering a unique approach to tuning coherent spin-spin interactions, this direct experimental determination of $\langle|\Delta B_{\mathrm{hyp}}|\rangle$ in the time domain is crucial to interpreting magnetic field effects in disordered organic semiconductors, noting prior controversy surrounding the precise value of $\langle|\Delta B_{\mathrm{hyp}}|\rangle$ [10]. This technique may also be of use for measuring differences in local magnetic environments in other materials where the g-factor separation is due to mechanisms other than the hyperfine field. Examples of nonhyperfine field mechanisms that could lead to different resonances of electron and hole include spin-orbit coupling [38], spin-dipolar coupling, and spin-exchange coupling [39] within the pair.

We note that determining $\langle|\Delta B_{\mathrm{hyp}}|\rangle$ by fitting the spectral line shapes assumed that there was no correlation between the hyperfine fields felt by polarons within each pair. The confirmation of this assumption by the time-domain beating indicates that there is no substantial overlap of the polaron wave functions, as such an overlap would lead to a correlation of the hyperfine fields from the nuclear spins within the shared region. This is consistent with the pairs having weak exchange, as confirmed by the B_1-field dependence of the Rabi frequency.

Spin-spin interactions in mesoscopic systems are usually investigated using coupled quantum dots, which are experimentally demanding [2,3,5,25]. Spin beating occurs naturally in organic semiconductors during bipolar carrier capture, the prerequisite process in any OLED. The combination of these versatile material systems with the unique abilities of the PEDMR technique promises many future insights into the fundamentals of spin interactions in small spin ensembles and may ultimately offer a hitherto unexplored pathway to creating entangled states for quantum information processing.

We appreciate many helpful discussions with Patrick Heissler. Acknowledgment is made to the Donors of the American Chemical Society Petroleum Research Fund (PRF48916-DNI10) and the Department of Energy (DE-SC0000909) for partial support of this research. We also thank the National Science Foundation (Grant No. CHE-ASC 0748473), and the David and Lucile Packard Foundation (J. M. L.) for financial support.

*lupton@physics.utah.edu
†boehme@physics.utah.edu

[1] N. M. Atherton, *Principles of Electron Spin Resonance* (Prentice Hall, New York, 1993).
[2] D. J. Reilly *et al.*, Science **321**, 817 (2008).
[3] H. O. H. Churchill *et al.*, Nature Phys. **5**, 321 (2009).
[4] G. Balasubramanian *et al.*, Nature Mater. **8**, 383 (2009).
[5] J. Petta *et al.*, Science **309**, 2180 (2005).
[6] S. Takahashi *et al.*, Phys. Rev. Lett. **101**, 047601 (2008).
[7] Y. Sheng *et al.*, Phys. Rev. B **74**, 045213 (2006).
[8] P. A. Bobbert *et al.*, Phys. Rev. Lett. **99**, 216801 (2007).
[9] M. Reufer *et al.*, Nature Mater. **4**, 340 (2005).
[10] J. M. Lupton and C. Boehme, Nature Mater. **7**, 598 (2008).
[11] J. D. Bergeson *et al.*, Phys. Rev. Lett. **100**, 067201 (2008).
[12] P. A. Bobbert *et al.*, Phys. Rev. Lett. **102**, 156604 (2009).
[13] W. H. Zurek, Rev. Mod. Phys. **75**, 715 (2003).
[14] D. R. McCamey *et al.*, Nature Mater. **7**, 723 (2008).
[15] C. Boehme and K. Lips, Phys. Rev. B **68**, 245105 (2003).
[16] V. Rajevac *et al.*, Phys. Rev. B **74**, 245206 (2006).
[17] Z. Xiong *et al.*, Nature (London) **427**, 821 (2004).
[18] V. A. Dediu *et al.*, Nature Mater. **8**, 707 (2009).
[19] W. M. Witzel and S. D. Sarma, Phys. Rev. B **77**, 165319 (2008).
[20] W. Harneit *et al.*, Phys. Rev. Lett. **98**, 216601 (2007).
[21] K. Tsukagoshi *et al.*, Nature (London) **401**, 572 (1999).
[22] N. Tombros *et al.*, Nature (London) **448**, 571 (2007).
[23] S. Kuroda *et al.*, Phys. Rev. Lett. **72**, 286 (1994).
[24] M. Pope and C. E. Swenberg, *Electronic Processes in Organic Crystals and Polymers* (Oxford University Press, New York, 1999).
[25] F. H. L. Koppens *et al.*, Science **309**, 1346 (2005).
[26] M. Segal *et al.*, Phys. Rev. B **68**, 075211 (2003).
[27] M. Wohlgennant *et al.*, Nature (London) **409**, 494 (2001).
[28] The spin resonance experiments were performed in a Bruker E580 pulsed EPR spectrometer. The devices were operated in forward bias at 1 mA.
[29] OLEDs were fabricated by spin coating a hole-injecting layer of poly(3,4-ethylenedioxythiophene) (PEDOT) and a layer of MEH-PPV. The PEDOT layer was contacted by an ITO electrode and the MEH-PPV by a Ca/Al layer.
[30] G. B. Silva *et al.*, Phys. Status Solidi C **2**, 3661 (2005).
[31] See supplementary material at http://link.aps.org/supplemental/10.1103/PhysRevLett.104.017601 for fit and further discussion.
[32] V. Dyakonov *et al.*, Phys. Rev. B **56**, 3852 (1997).
[33] C. Boehme *et al.*, Phys. Status Solidi B **246**, 2750 (2009).
[34] M.-K. Lee *et al.*, Phys. Rev. Lett. **94**, 137403 (2005).
[35] Rabi oscillations were measured by monitoring the current transient 7.4 μs after the microwave pulse, on the maximum of the resonance, as a function of pulse length. The Rabi oscillations appear on a single-exponential transient approaching the on-resonance steady state, which was subtracted to obtain the data in Fig. 2(b).
[36] The relative contribution of the two frequency components, $f(\Omega)$, shown in Fig. 3(b), was found noting that $f(\Omega_{\mathrm{Rabi}}) = A(\Omega_{\mathrm{Rabi}})/[A(\Omega_{\mathrm{Rabi}}) + 2A(2\Omega_{\mathrm{Rabi}})]$, and $f(2\Omega_{\mathrm{Rabi}}) = 1 - f(\Omega_{\mathrm{Rabi}})$, where $A(X)$ is the value of the Fourier transform at frequency X. The beating value is multiplied by 2, as the beat oscillation contributes only half the change in current [15,16]. We note that the state $\frac{1}{2}(|\uparrow\rangle + |\downarrow\rangle) \otimes (|\uparrow\rangle + |\downarrow\rangle) = \frac{1}{2}|T_+\rangle + \frac{1}{2}|T_-\rangle + \frac{1}{\sqrt{2}}|T_0\rangle$ is a triplet noneigenstate, a component of which oscillates rapidly between $|T_0\rangle$ and $|S_0\rangle$ after its creation.
[37] K. Lips *et al.*, J. Optoelectron. Adv. Mater. **7**, 13 (2005).
[38] J. M. Spaeth and H. Overhof, *Point Defects in Semiconductors and Insulators* (Springer, Berlin, 2003).
[39] S. Schaefer *et al.*, Phys. Status Solidi B **245**, 2120 (2008).